Steinbach, J. H., & Ifune, C. (1989) *Trends Neurosci. 12*, 3–6.
Takashaki, K. (1968) *J. Biol. Chem. 243*, 6171–6179.
Vázquez, J., García-Calvo, M., Valdivieso, F., Mayor, F., & Mayor, F., Jr. (1988) *J. Biol. Chem. 263*, 1255–1265.
Young, A. B., & Snyder, S. H. (1973) *Proc. Natl. Acad. Sci. U.S.A. 70*, 2832–2836.
Young, A. B., & Snyder, S. H. (1974) *Mol. Pharmacol. 10*, 790–809.

Existence of a Low-Affinity ATP-Binding Site in the Unphosphorylated Ca^{2+}-ATPase of Sarcoplasmic Reticulum Vesicles: Evidence from Binding of 2′,3′-*O*-(2,4,6-Trinitrocyclohexadienylidene)-[^{3}H]AMP and -[^{3}H]ATP†

Hiroshi Suzuki,‡ Tatsuya Kubota,‡,§ Koji Kubo,‡,§ and Tohru Kanazawa*,‡
Department of Biochemistry and Third Department of Internal Medicine, Asahikawa Medical College, Asahikawa 078, Japan
Received March 1, 1990; Revised Manuscript Received April 20, 1990

ABSTRACT: ATP-binding sites in the unphosphorylated Ca^{2+}-ATPase of sarcoplasmic reticulum vesicles were titrated with 2′,3′-*O*-(2,4,6-trinitrocyclohexadienylidene)-[^{3}H]AMP (TNP-AMP) or -[^{3}H]ATP (TNP-ATP) in the absence of Ca^{2+} at pH 7.0 and 0 °C by using a centrifugation procedure. In some measurements, the bound TNP-nucleotides were chased with ATP. The data were analyzed by best-fit computer programs as well as by Scatchard plots. The results showed the existence of 1 mol of TNP-AMP binding sites with high affinity (K_d = 7.62 nM) per mole of phosphorylatable sites. The affinity of these sites for ATP (K_d = 10.1 μM) agreed with that of catalytic sites for ATP in the absence of Ca^{2+}. The results further showed the existence of 2 mol of TNP-ATP binding sites with uniform affinity (K_d = 156 nM) per mole of phosphorylatable sites. Half of the bound TNP-ATP was fully chased by low concentrations of ATP. The affinity of this class of the sites for ATP (K_d = 8.9 μM) again agreed with that of catalytic sites for ATP. The other half of the bound TNP-ATP was fully chased only by much higher concentrations of ATP. Thus, the affinity of this class of the sites for ATP (K_d = 791 μM) was much lower than that of catalytic sites for ATP. Similar measurements were performed with sarcoplasmic reticulum vesicles pretreated by *N*-(iodoacetyl)-*N*′-(5-sulfo-1-naphthyl)ethylenediamine. Although the affinities for TNP-ATP and for ATP were appreciably altered by this pretreatment, the results were essentially the same as those obtained with native vesicles. These results demonstrate that, in the unphosphorylated enzyme, there exists 1 mol of low-affinity ATP-binding sites as well as 1 mol of high-affinity ATP-binding sites (catalytic sites) per mole of phosphorylatable sites.

The membrane-bound Ca^{2+}-ATPase of sarcoplasmic reticulum catalyzes the active Ca^{2+} transport coupled to ATP hydrolysis (Hasselbach & Makinose, 1961; Ebashi & Lipmann, 1962). The enzyme consists of a 110-kDa single polypeptide chain (Brandl et al., 1986) that has one catalytic site with a high affinity for ATP (Meissner, 1973; Dupont, 1977; Mitchinson et al., 1982; Inesi et al., 1982).

The ATPase activity is modulated by ATP in a complex manner, so that it exhibits non-Michaelian behavior with respect to ATP (Inesi et al., 1967; Yamamoto & Tonomura, 1967; Dupont, 1977; Verjovski-Almeida & Inesi, 1979). It has been shown that several steps in the catalytic cycle are accelerated by ATP binding to a putative regulatory site(s) at concentrations higher than those required for saturation of the catalytic site (Yamamoto & Tonomura, 1967; de Meis & de Mello, 1973; Froehlich & Taylor, 1975; Scofano et al., 1979; McIntosh & Boyer, 1983). These regulations are due to nonhydrolytic effects of ATP because the accelerations can be also induced by nonhydrolyzable ATP analogues (Dupont, 1977; Taylor & Hattan, 1979; McIntosh & Boyer, 1983; Dupont et al., 1985; Champeil et al., 1988; Seebregts & McIntosh, 1989).

It has been well documented that hydrolysis of EP[1] is modulated by ATP binding to the catalytic site of EP after the departure of ADP (McIntosh & Boyer, 1983; Bishop et al., 1987; Champeil et al., 1988; Seebregts & McIntosh, 1989). On the other hand, there are accumulating observations to suggest that ATP-induced regulations may be due to interaction between two distinct classes of ATP-binding sites or to dimeric interaction between two catalytic sites in the subunits (Ikemoto, 1982; Dupont et al., 1982; Carvalho-Alves et al., 1985; Dupont et al., 1985; Ferreira & Verjovski-Almeida, 1988). However, no convincing evidence for the existence of regulatory ATP-binding sites other than the catalytic site of EP has been presented so far.

One of the main obstacles to conclusive evidence for these regulatory sites is the difficulty of direct titration by ATP due

† This work was supported in part by a Grant-in-Aid for Scientific Research on Priority Areas of "Bioenergetics" to T. Kanazawa and in part by a Grant-in-Aid to H. Suzuki from the Ministry of Education, Science and Culture, Japan.
* Address correspondence to this author.
‡ Department of Biochemistry.
§ Third Department of Internal Medicine.

[1] Abbreviations: EP, phosphoenzyme; SRV, sarcoplasmic reticulum vesicles; TNP-AMP, 2′,3′-*O*-(2,4,6-trinitrocyclohexadienylidene)-AMP; TNP-ATP, 2′,3′-*O*-(2,4,6-trinitrocyclohexadienylidene)-ATP; I-EDANS, *N*-(iodoacetyl)-*N*′-(5-sulfo-1-naphthyl)ethylenediamine; EDANS, *N*-acetyl-*N*′-(5-sulfo-1-naphthyl)ethylenediamine; Tris, tris(hydroxymethyl)aminomethane; MOPS, 3-(*N*-morpholino)propanesulfonic acid; EGTA, [ethylenebis(oxyethylenenitrilo)]tetraacetic acid.

0006-2960/90/0429-7040$02.50/0

to the predicted low affinity for ATP (Inesi et al., 1967; Yamamoto & Tonomura, 1967; Dupont, 1977; McIntosh & Boyer, 1983). Previously, Dupont et al. (1985) tried to titrate regulatory sites using fluorescent nonhydrolyzable ATP analogues, TNP-nucleotides, as these analogues were shown to bind to nucleotide binding sites with very high affinity (Dupont et al., 1982). From the findings in the ATP-induced chase of TNP-nucleotides, the authors suggested the existence of low-affinity ATP-binding sites. However, the evidence was not conclusive since, in their fluorescence measurements, the ATP-induced chase was limited by an inevitable dilution artifact due to addition of high concentrations of Mg·ATP and as a result the full chase was not achieved.

In the present work, we have titrated ATP-binding sites with TNP-[^{3}H]AMP or TNP-[^{3}H]ATP using centrifugation procedures followed by radioactivity measurements. The bound TNP-[^{3}H]AMP and TNP-[^{3}H]ATP have been almost completely chased by added ATP with no appreciable artifact. The results thus obtained clearly demonstrate that, in the unphosphorylated enzyme, there exists 1 mol of low-affinity ATP-binding sites as well as 1 mol of high-affinity ATP-binding sites (catalytic sites) per mole of phosphorylatable sites.

Experimental Procedures

Materials. ATP was purchased from Boehringer Mannheim. I-EDANS was obtained from Aldrich. [2-^{3}H]AMP and [2,8-^{3}H]ATP were from Amersham and ICN Biochemicals Inc., respectively. TNP-[^{3}H]AMP and TNP-[^{3}H]ATP were synthesized according to Hiratsuka (1982) using [2-^{3}H]AMP and [2,8-^{3}H]ATP. [γ-^{32}P]ATP was prepared by the method of Post and Sen (1967). Protein concentrations were determined according to Lowry et al. (1951) with bovine serum albumin as a standard.

Preparation of Native SRV. Native SRV were prepared from rabbit skeletal muscle as described previously (Kanazawa et al., 1971) and stored in 0.3 M sucrose, 0.1 mM $CaCl_2$, 0.1 M KCl, and 5 mM MOPS–Tris (pH 7.0) at −80 °C.

Treatment of Native SRV with I-EDANS. Treatment of native SRV with I-EDANS was performed as described previously (Suzuki et al., 1987). Activities of ATP hydrolysis and Ca^{2+} transport were not substantially impaired by this treatment, as compared to native SRV.

Measurements of Binding of TNP-[^{3}H]AMP or TNP-[^{3}H]ATP. Native SRV or EDANS-SRV were suspended in 20 mM MOPS–Tris (pH 7.0) containing 2 mM EGTA, 10 mM $MgCl_2$, 0.1 M KCl, and different concentrations of either TNP-[^{3}H]AMP or TNP-[^{3}H]ATP. After incubation at 0 °C for 15 min, the suspension was centrifuged at 541000g for 20 min at 0 °C in an ultracentrifuge (Hitachi, HIMAC CP100H). In some measurements, a small volume of ATP was added 10 min after the start of incubation. The resulting suspension had a composition of 20 mM MOPS–Tris (pH 7.0), 2 mM EGTA, 10 mM $MgCl_2$, 0.1 M KCl, a given concentration of either TNP-[^{3}H]AMP or TNP-[^{3}H]ATP, and different concentrations of ATP. The suspension was further incubated for 15 min at 0 °C for equilibration and then centrifuged as described above. The temperature was monitored during the spin, and its change was found to be within 1 °C throughout. More than 98% of native SRV and EDANS-SRV were sedimented as judged from protein concentrations and from fluorescence intensities of bound EDANS in the supernatants. The concentration of free TNP-[^{3}H]AMP or free TNP-[^{3}H]ATP was obtained from the radioactivity of the supernatant. The amount of bound TNP-[^{3}H]AMP or bound TNP-[^{3}H]ATP was obtained from the difference in radioactivity between the suspension before centrifugation and the supernatant after centrifugation.

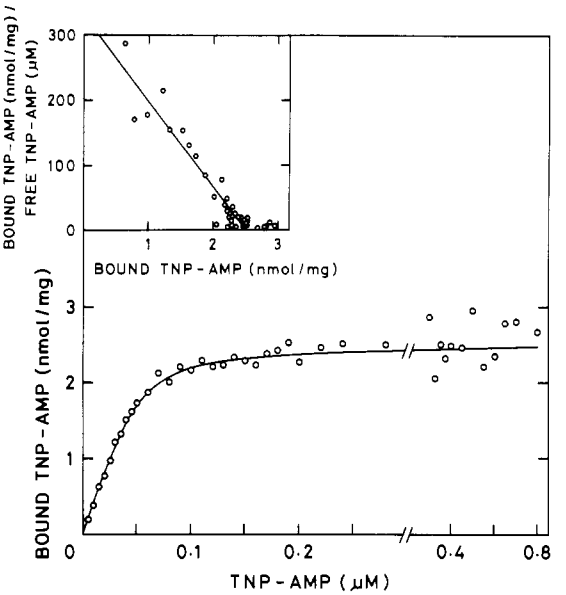

FIGURE 1: Binding of TNP-AMP to native SRV. Native SRV (20.0 μg of protein/mL) were incubated with different concentrations of TNP-[^{3}H]AMP as indicated on the abscissa, and the amounts of bound TNP-[^{3}H]AMP were measured. From a linear regression of the Scatchard plot in the inset, the dissociation constant (K_1) and the number of binding sites (N) were estimated to be 7.62 nM and 2.50 nmol of binding sites/mg of protein, respectively. The solid line represents a simulation deduced on the assumption that TNP-AMP binds to homogeneous sites with K_1 and N as estimated above.

Analyses of Binding Data. For TNP-[^{3}H]AMP binding, Scatchard plots were analyzed by least-squares fit to a straight line. For TNP-[^{3}H]ATP binding as well as for ATP-induced chase of bound TNP-[^{3}H]AMP or TNP-[^{3}H]ATP, data were analyzed by using a FORTRAN program according to Marquardt's algorithm (Marquardt, 1963) which combines the gradient search with the method of linearizing the fitting function for least-squares estimation of nonlinear parameters [see pp 235–242 in Bevington's textbook (Bevington, 1969) for details of this FORTRAN program].

Determination of EP. Phosphorylation of native SRV or EDANS-SRV was carried out with [γ-^{32}P]ATP according to Barrabin et al. (1984). The amount of EP was determined as described previously (Takakuwa & Kanazawa, 1982).

Results

Binding of TNP-AMP to Native SRV. Binding of TNP-AMP to native SRV was determined at different TNP-AMP concentrations (Figure 1). The binding was saturated at very low concentrations of TNP-AMP. The Scatchard plot was approximately linear (the inset of Figure 1), and the least-squares fit to a straight line revealed the existence of 2.50 nmol of homogeneous binding sites/mg of protein with a dissociation constant of 7.62 nM. The level of EP determined as described under Experimental Procedures was 2.02 nmol/mg of protein. Since the total number of phosphorylatable catalytic sites is 10–15% higher than this EP level (see Discussion), these results indicate that there exists 1 mol of high-affinity TNP-AMP binding sites per mole of phosphorylatable catalytic sites in native SRV.

ATP-Induced Chase of TNP-AMP Bound to Native SRV. Native SRV (this preparation gave 2.02 nmol of EP/mg of protein) were incubated with TNP-AMP, and then the bound TNP-AMP was chased by addition of different concentrations of ATP (Figure 2). The bound TNP-AMP decreased with increasing ATP concentration and was almost completely

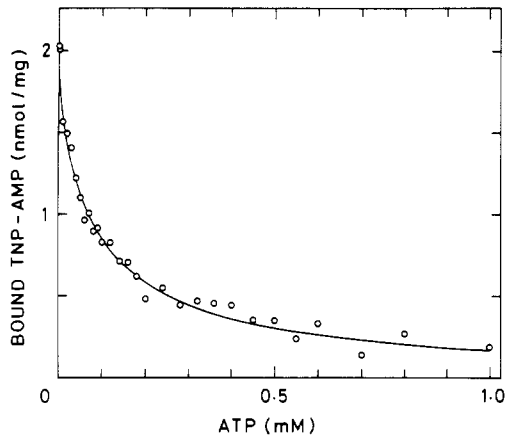

FIGURE 2: ATP-induced chase of TNP-AMP bound to native SRV. Native SRV were incubated with TNP-[^{3}H]AMP, and then the bound TNP-[^{3}H]AMP was chased by addition of different concentrations of ATP. The final concentrations of native SRV, TNP-[^{3}H]AMP, and ATP were 20.0 μg of protein/mL (50.0 nM TNP-AMP binding sites), 60.0 nM, and concentrations indicated on the abscissa, respectively. The assumption of competitive binding of TNP-[^{3}H]AMP and ATP to homogeneous independent sites leads to eq 1, where N,

$$[ES] = \{(N + S + K_1 + IK_1/K_2) - [(N + S + K_1 + IK_1/K_2)^2 - 4NS]^{1/2}\}/2 \quad (1)$$

[ES], S, and I denote concentrations of TNP-AMP binding sites, bound TNP-[^{3}H]AMP, added TNP-[^{3}H]AMP, and free ATP, respectively. K_1 and K_2 signify dissociation constants of the sites for TNP-[^{3}H]AMP and ATP, respectively. By the best fit to eq 1 using N (50.0 nM) and K_1 estimated in Figure 1 as well as using concentrations of added ATP as an approximation of I, K_2 was estimated to be 10.1 μM. The solid line represents a simulation deduced from eq 1 with these parameters.

chased by 1 mM ATP. The estimated dissociation constant for ATP (10.1 μM) agreed with the previously reported affinity of catalytic sites for ATP in the absence of Ca^{2+} (Meissner, 1973; Dupont, 1977). This indicates that TNP-AMP exclusively binds to catalytic sites under the given conditions.

Binding of TNP-ATP to Native SRV. Binding of TNP-ATP to native SRV (this preparation gave 2.02 nmol of EP/mg of protein) was determined at different TNP-ATP concentrations (Figure 3). Since the amount of bound TNP-ATP at saturating concentrations was approximately twice as large as that of bound TNP-AMP (cf. Figure 1), it was assumed that there exist two classes of TNP-ATP binding sites (sites 1 and 2) equal in number. The results of the best fit to eq 2 deduced from this assumption (see the legend for Figure 3) and the observed excellent fit of the simulation strongly suggest that the enzyme has 2 mol of TNP-ATP binding sites/mol of phosphorylatable catalytic sites and that these sites have a uniform affinity for TNP-ATP. The Scatchard plot (the inset of Figure 3) gave a single straight line with a slope of -6.41 μM^{-1} having no break and an intercept of 4.46 nmol of binding sites/mg of protein on the abscissa. This finding is consistent with the above conclusion deduced from the best fit to eq 2.

ATP-Induced Chase of TNP-ATP Bound to Native SRV. Native SRV (this preparation gave 2.02 nmol of EP/mg of protein) were incubated with TNP-ATP, and then the bound TNP-ATP was chased by addition of different concentrations of ATP (Figure 4). Half of the bound TNP-ATP was fully chased by low concentrations of ATP, whereas the other half of the bound TNP-ATP was fully chased only when ATP concentrations were much higher. The dissociation constants of sites 1 and 2 for ATP were estimated to be 8.9 and 791 μM, respectively. Thus, the affinity of site 1 for ATP agreed with the affinity of catalytic sites for ATP in the absence of Ca^{2+}.

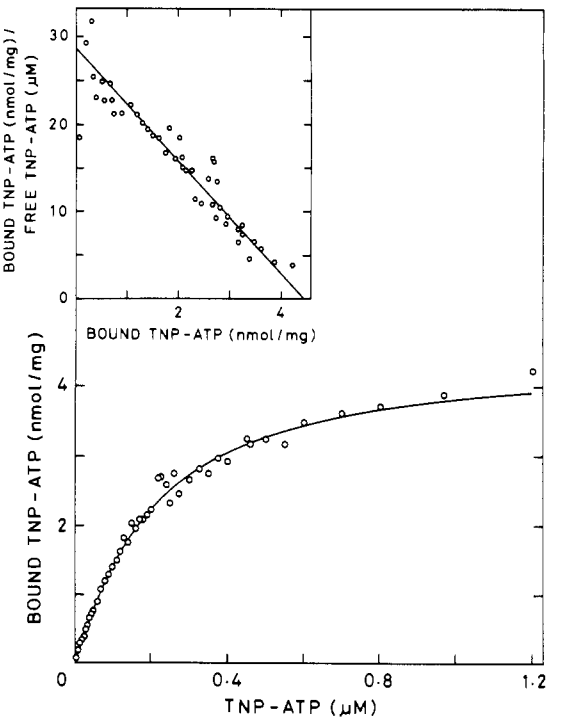

FIGURE 3: Binding of TNP-ATP to native SRV. Native SRV (20.0 μg of protein/mL) were incubated with different concentrations of TNP-[^{3}H]ATP as indicated on the abscissa, and the amounts of bound TNP-[^{3}H]ATP were measured. The assumption of the existence of two classes of independent binding sites (sites 1 and 2) equal in number leads to eq 2, where N, [ES], and S denote the number of site 1 (or

$$[ES] = N/(1 + K_1/S) + N/(1 + K_2/S) \quad (2)$$

site 2), the amount of bound TNP-[^{3}H]ATP, and the concentration of free TNP-[^{3}H]ATP, respectively. K_1 and K_2 signify dissociation constants for TNP-[^{3}H]ATP of sites 1 and 2, respectively. By the best fit to eq 2, K_1, K_2, and N were estimated to be 156 nM, 156 nM, and 2.23 nmol of binding sites/mg of protein, respectively. The Scatchard plot is shown in the inset. The solid lines represent simulations deduced from eq 2 with the parameters estimated above.

In contrast, the affinity of site 2 for ATP was much lower than that of catalytic sites for ATP. These findings show that there exists 1 mol of low-affinity ATP-binding sites as well as 1 mol of high-affinity ATP-binding sites per mole of phosphorylatable catalytic sites in native SRV.

Binding of TNP-AMP to EDANS-SRV. As shown later, we found unexpectedly that affinities of the sites for TNP-ATP were appreciably modified by the I-EDANS treatment. Fortunately, this allowed us to directly distinguish site 2 from site 1 without the ATP-induced chase. For this reason, binding measurements were performed with EDANS-SRV in the following experiment. First, binding of TNP-AMP to EDANS-SRV was determined at different TNP-AMP concentrations under the same conditions as described in Figure 1 except for 70.0 μg of protein of EDANS-SRV/mL (not shown). The binding showed a saturation in the concentration range from 0.3 to 1.0 μM TNP-AMP. The Scatchard plot was again linear, giving 3.00 nmol of homogeneous binding sites/mg of protein with a dissociation constant of 7.27 nM. With this preparation of EDANS-SRV used, the level of EP was found to be 2.27 nmol/mg. These observations show the existence of 1 mol of high-affinity TNP-AMP binding sites/mol of phosphorylatable catalytic sites. This finding is essentially the same as that obtained with native SRV (cf. Figure 1).

ATP-Induced Chase of TNP-AMP Bound to EDANS-SRV. EDANS-SRV (this preparation gave 2.27 nmol of EP/mg of protein) were incubated with TNP-AMP, and then

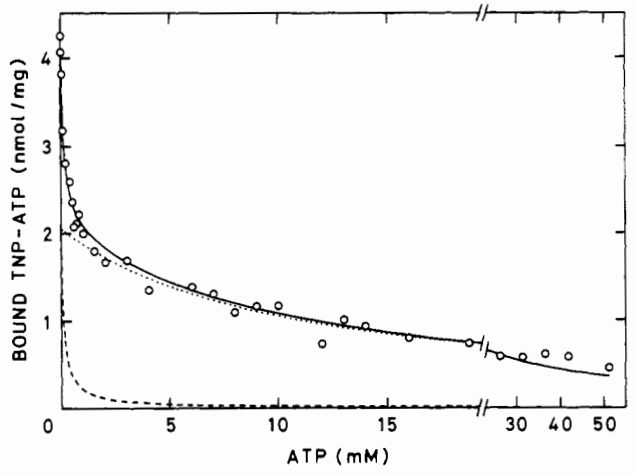

FIGURE 4: ATP-induced chase of TNP-ATP bound to native SRV. Native SRV were incubated with TNP-[^{3}H]ATP, and then the bound TNP-[^{3}H]ATP was chased by addition of different concentrations of ATP. The final concentrations of native SRV, TNP-[^{3}H]ATP, and ATP were 70.0 μg of protein/mL [156 nM site 1 (or site 2)], 2.00 μM, and concentrations indicated on the abscissa, respectively. The assumption of competitive binding of TNP-[^{3}H]ATP and ATP to independent sites (sites 1 and 2) leads to eq 3, where N, [ES], S,

$$[ES] = N/[1 + K_1/S + K_1I/(K_3S)] + N/[1 + K_2/S + K_2I/(K_4S)] \quad (3)$$

K_1, and K_2 have the same meanings as in Figure 3. I designates the concentration of free ATP. K_3 and K_4 denote dissociation constants for ATP of sites 1 and 2, respectively. By the best fit to eq 3 using K_1, K_2, and N estimated in Figure 3 as well as using concentrations of added ATP as an approximation of I, K_3 and K_4 were estimated to be 8.9 and 791 μM, respectively. The solid, broken, and dotted lines represent simulations deduced from eq 3, the first term of eq 3, and the second term of eq 3, respectively, with the above parameters.

the bound TNP-AMP was chased by addition of different concentrations of ATP (not shown). The final concentrations of EDANS-SRV and TNP-AMP were 20.0 μg of protein/mL (60.0 nM TNP-AMP binding sites) and 100 nM, respectively. The bound TNP-AMP decreased with increasing ATP concentration, and almost all the bound TNP-AMP was chased with 2.5 mM ATP. By the best fit to eq 1 given in the legend for Figure 2 using the concentration of binding sites (N = 60.0 nM) and the dissociation constant for TNP-AMP (K_1 = 7.27 nM) estimated above as well as using concentrations of added ATP as an approximation of the concentration of free ATP (I), the dissociation constant for ATP (K_2) was estimated to be 13.9 μM. This value agreed with the affinity of catalytic sites for ATP in the absence of Ca^{2+}. These findings again strongly suggest that the TNP-AMP binding sites are actually catalytic sites.

Binding of TNP-ATP to EDANS-SRV. The binding of TNP-ATP to EDANS-SRV (this preparation gave 2.72 nmol of EP/mg of protein) was determined at different TNP-ATP concentrations (Figure 5A). Since the amount of bound TNP-ATP at saturating TNP-ATP concentrations was approximately twice as large as that of bound TNP-AMP, it was again assumed that there exist two classes of TNP-ATP binding sites (sites 1 and 2) equal in number. The results of the best fit to eq 2 and the excellent fit of the simulation indicate that there exists 2 mol of TNP-ATP binding sites/mol of phosphorylatable catalytic sites and that the affinity for TNP-ATP of site 1 is 6–7 times as high as that of site 2. This difference in the affinity between sites 1 and 2 with EDANS-SRV is in contrast to the observed equality of the affinity between sites 1 and 2 with native SRV (cf. Figure 3).

The Scatchard plot of TNP-ATP binding to EDANS-SRV was not linear (Figure 5B). This is consistent with the above

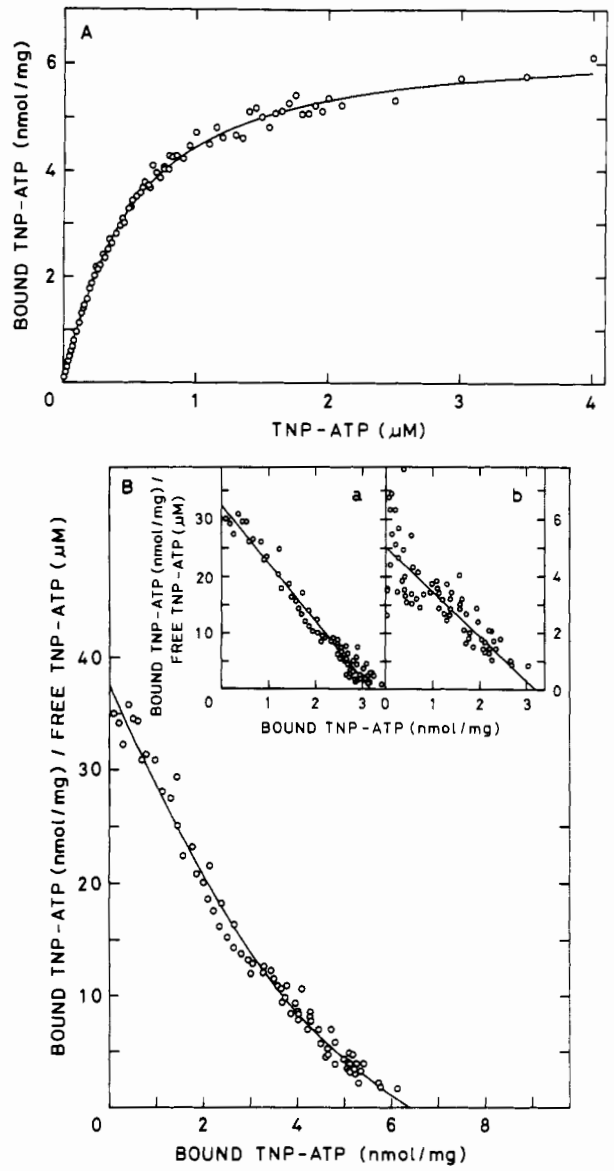

FIGURE 5: Binding of TNP-ATP to EDANS-SRV. (A) EDANS-SRV (70.0 μg of protein/mL) were incubated with different concentrations of TNP-[^{3}H]ATP as indicated on the abscissa, and the amounts of bound TNP-[^{3}H]ATP were measured. The assumption of the existence of two classes of independent binding sites (sites 1 and 2) equal in number leads to eq 2 given in the legend for Figure 3. By the best fit to eq 2, K_1, K_2, and N were estimated to be 98.5 nM, 637 nM, and 3.20 nmol of binding sites/mg of protein, respectively. The solid line represents a simulation deduced from eq 2 with the parameters estimated above. (B) The Scatchard plot of the binding data in (A) is shown. The solid line represents a simulation which is deduced from eq 2 with the parameters estimated in (A). (Inset a) The Scatchard plot of TNP-[^{3}H]ATP binding is made after subtraction of the amounts of bound TNP-[^{3}H]ATP calculated from the second term of eq 2. The solid line represents a simulation deduced from the first term of eq 2. (Inset b) The Scatchard plot of TNP-[^{3}H]ATP binding is made after subtraction of the amounts of bound TNP-[^{3}H]ATP calculated from the first term of eq 2. The solid line represents a simulation deduced from the second term of eq 2.

conclusion, again indicating that the TNP-ATP binding sites are not homogeneous. The Scatchard plot after subtraction of theoretical amounts of TNP-ATP bound to site 2 was linear and revealed the existence of 3.20 nmol of site 1/mg of protein with a dissociation constant of 98.5 nM (inset a of Figure 5B). The Scatchard plot after subtraction of theoretical amounts of TNP-ATP bound to site 1 was also approximately linear and revealed the existence of 3.20 nmol of site 2/mg of protein with a dissociation constant of 637 nM (inset b of Figure 5B).

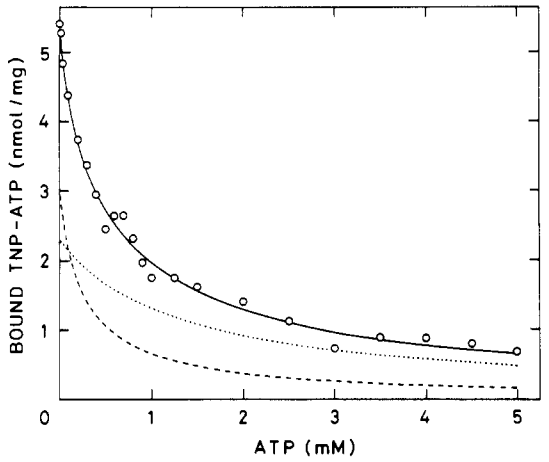

FIGURE 6: ATP-induced chase of TNP-ATP bound to EDANS-SRV. EDANS-SRV were incubated with TNP-[^{3}H]ATP, and then the bound TNP-[^{3}H]ATP was chased by addition of different concentrations of ATP. The final concentrations of EDANS-SRV, TNP-[^{3}H]ATP, and ATP were 70.0 μg of protein/mL [224 nM site 1 (or site 2)], 2.00 μM, and concentrations indicated on the abscissa. The assumption of competitive binding of TNP-[^{3}H]ATP and ATP to independent sites (sites 1 and 2) leads to eq 3 given in the legend for Figure 4. By the best fit to eq 3 using K_1, K_2, and N estimated in Figure 5A as well as using concentrations of added ATP as an approximation of I, K_3 and K_4 were estimated to be 13.9 and 312 μM, respectively. The solid, broken, and dotted lines represent simulations deduced from eq 3, the first term of eq 3, and the second term of eq 3, respectively, with the above parameters.

All these findings demonstrate that there exists 1 mol of low-affinity TNP-ATP binding sites (site 2) as well as 1 mol of high-affinity TNP-ATP binding sites (site 1) per mole of phosphorylatable catalytic sites in EDANS-SRV.

ATP-Induced Chase of TNP-ATP Bound to EDANS-SRV. EDANS-SRV (this preparation gave 2.72 nmol of EP/mg of protein) were incubated with TNP-ATP, and then the bound TNP-ATP was chased by addition of different concentrations of ATP (Figure 6). The dissociation constants for ATP of sites 1 and 2 were estimated to be 13.9 and 312 μM, respectively. Thus, the affinity of site 1 for ATP agreed reasonably with the affinity of catalytic sites for ATP in the absence of Ca^{2+}. On the other hand, the affinity of site 2 for ATP was much lower than that of catalytic sites for ATP. This conclusion is essentially the same as that obtained with native SRV although affinities of these sites for TNP-ATP and ATP were appreciably modified by the I-EDANS treatment.

Discussion

The present results demonstrate that there exists 1 mol of low-affinity ATP-binding sites as well as 1 mol of high-affinity ATP-binding sites per mole of phosphorylatable catalytic sites in the unphosphorylated Ca^{2+}-ATPase of SRV.

In this study, the number 10–15% higher than the level of EP formed from ATP according to Barrabin et al. (1984) has been used as a reasonable estimate of the total number of phosphorylatable catalytic sites because of the steady-state character of this EP level. The reliability of this estimation has been well documented by Inesi and co-workers (Inesi et al., 1982; Barrabin et al., 1984).

One might suspect that the observed low-affinity ATP-binding sites are derived from the deteriorated catalytic sites in the partially denatured Ca^{2+}-ATPase or from contaminant proteins possibly having low-affinity ATP-binding sites. However, these possibilities are unlikely because the stoichiometry of 1 mol of the low-affinity ATP-binding sites/mol of phosphorylatable catalytic sites is consistently obtained with different preparations of SRV. This is typically shown by the finding that the stoichiometry is retained even when the level of EP fluctuates from 2.02 nmol of EP/mg of protein (Figures 3 and 4) to 2.72 nmol of EP/mg of protein (Figures 5 and 6).

The finding that 1 mol of TNP-AMP/mol of phosphorylatable catalytic sites binds to SRV (native SRV and EDANS-SRV) with very high affinity (see Figure 1 and text) is consistent with the results previously reported by Bishop et al. (1987) and by Seebregts and McIntosh (1989). The finding that 2 mol of TNP-ATP/mol of phosphorylatable catalytic sites binds to SRV (native SRV and EDANS-SRV) (Figures 3 and 5) is also compatible with the results previously reported by Watanabe and Inesi (1982) and by Dupont et al. (1982, 1985). However, the observed affinity for TNP-ATP in the present experiment is much higher than that reported by Watanabe and Inesi (1982). This discrepancy remains unsolved but may possibly be due to the difference in SRV concentrations used. Actually, we used 0.02 mg of protein/mL and found a single dissociation constant of 0.156 μM with native SRV, whereas Watanabe and Inesi used 0.8 mg of protein/mL and found two different dissociation constants of 1.5 and 160 μM with native SRV.

As stated above, for TNP-ATP binding to native SRV (Figure 3), we found a single dissociation constant from the best-fit analysis of binding data and from the linearity of the Scatchard plot. Although this appears to suggest that TNP-ATP binding sites might be homogeneous, it does not exclude the possibility that these sites are actually heterogeneous. In fact, the ATP-induced chase of bound TNP-ATP (Figure 4) reveals that the TNP-ATP binding sites consist of two populations having greatly different affinities for ATP. Dupont et al. (1985) previously tried to perform the ATP-induced chase of a bound TNP-ATP analogue in the fluorometric measurements and obtained findings suggestive of two distinct classes of nucleotide binding sites. However, the second part of this chase (possibly corresponding to low-affinity ATP-binding sites) was not fully observed since it was difficult to use high concentrations of Mg·ATP for the chase without a dilution artifact. On the other hand, in the present experiment, the evidence for two distinct classes of TNP-ATP binding sites has been directly obtained without the ATP-induced chase by using EDANS-SRV in place of native SRV (Figure 5).

Previously, in photoaffinity labeling with 3′-(arylazido)-ATP, Carvalho-Alves et al. (1985) suggested the existence of two distinct low- and high-affinity nucleotide sites. However, the observed levels of labeling are too high (6.5–9.0 nmol of label/mg of protein in binding to the high-affinity sites and 20–22 nmol of label/mg of protein in binding to both the low- and high-affinity sites), being inconsistent with our present results and also quite incompatible with the previously reported concentration of catalytic sites (Barrabin et al., 1984; Gafni & Boyer, 1984).

It is not clear at present whether the observed low- and high-affinity ATP-binding sites exist on a single polypeptide chain of the enzyme or the low-affinity ATP-binding sites are derived from catalytic sites modulated by a possible dimeric interaction. In the present analysis, it is assumed that binding sites are independent. However, this does not exclude the possibility of dimeric interaction. A number of findings in favor of dimeric interaction have been reported (Ikemoto, 1982; Dupont et al., 1985). Recently, Ferreira and Verjovski-Almeida (1988) have found that a maximum level of EP formed from UTP is twice as high as that of EP formed from ATP, suggesting half-of-the-sites reactivity induced by dimeric interaction in the presence of ATP. On the other hand, unfavorable findings for half-of-the sites reactivity have also been

reported by many authors (Bishop et al., 1987; Champeil et al., 1988; Seebregts & McIntosh, 1989). Indeed, a dimeric interaction is still a matter of controversy.

Quite recently, by using spin-labeled 2-azido-ATP, Jakobs et al. (1989) obtained ESR spectra indicative of distinct and possibly adjacent ATP-binding sites. It is unknown whether these sites are the same as those revealed in the present experiment. For definite characterization of the observed low-affinity ATP-binding sites, it may be important to locate the sites on the primary structure of the enzyme.

At present we have no evidence for functional roles of the low-affinity ATP-binding sites shown in the present experiment. However, it is possible that these sites have a role in modulation of the catalytic activity in some reaction step. This possible functional role should be revealed in further investigation.

ACKNOWLEDGMENTS

T. Kubota and K. Kubo are grateful to Prof. Masayoshi Namiki (Third Department of Internal Medicine, Asahikawa Medical College) for his continued encouragement during this work.

REFERENCES

Barrabin, H., Scofano, H. M., & Inesi, G. (1984) *Biochemistry 23*, 1542–1548.

Bevington, P. R. (1969) *Data Reduction and Error Analysis for the Physical Sciences*, pp 235–242, McGraw-Hill Book Co., New York.

Bishop, J. E., Al-Shawi, M. K., & Inesi, G. (1987) *J. Biol. Chem. 262*, 4658–4663.

Brandl, C. J., Green, N. M., Korczak, B., & MacLennan, D. H. (1986) *Cell 44*, 597–607.

Carvalho-Alves, P. C., Oliveira, C. R. G., & Verjovski-Almeida, S. (1985) *J. Biol. Chem. 260*, 4282–4287.

Champeil, P., Riollet, S., Orlowski, S., Guillain, F., Seebregts, C. J., & McIntosh, D. B. (1988) *J. Biol. Chem. 263*, 12288–12294.

de Meis, L., & de Mello, M. C. F. (1973) *J. Biol. Chem. 248*, 3691–3701.

Dupont, Y. (1977) *Eur. J. Biochem. 72*, 185–190.

Dupont, Y., Chapron, Y., & Pougeois, R. (1982) *Biochem. Biophys. Res. Commun. 106*, 1272–1279.

Dupont, Y., Pougeois, R., Ronjat, M., & Verjovski-Almeida, S. (1985) *J. Biol. Chem. 260*, 7241–7249.

Ebashi, S., & Lipmann, F. (1962) *J. Cell Biol. 14*, 389–400.

Ferreira, S. T., & Verjovski-Almeida, S. (1988) *J. Biol. Chem. 263*, 9973–9980.

Froehlich, J. P., & Taylor, E. W. (1975) *J. Biol. Chem. 250*, 2013–2021.

Gafni, A., & Boyer, P. D. (1984) *Biochemistry 23*, 4362–4367.

Hasselbach, W., & Makinose, M. (1961) *Biochem. Z. 333*, 518–528.

Hiratsuka, T. (1982) *Biochim. Biophys. Acta 719*, 509–517.

Ikemoto, N. (1982) *Annu. Rev. Physiol. 44*, 297–317.

Inesi, G., Goodman, J. J., & Watanabe, S. (1967) *J. Biol. Chem. 242*, 4637–4643.

Inesi, G., Watanabe, T., Coan, C., & Murphy, A (1982) *Ann. N.Y. Acad. Sci. 402*, 515–534.

Jakobs, P., Sauer, H. E., McIntyre, J. O., Fleischer, S., & Trommer, W. E. (1989) *FEBS Lett. 254*, 8–12.

Kanazawa, T., Yamada, S., Yamamoto, T., & Tonomura, Y. (1971) *J. Biochem. (Tokyo) 70*, 95–123.

Lowry, O. H., Rosebrough, N. J., Farr, A. L., & Randall, R. J. (1951) *J. Biol. Chem. 193*, 265–275.

Marquardt, D. W. (1963) *J. Soc. Ind. Appl. Math. 11*, 431–441.

McIntosh, D. B., & Boyer, P. D. (1983) *Biochemistry 22*, 2867–2875.

Meissner, G. (1973) *Biochim. Biophys. Acta 298*, 906–926.

Mitchinson, C., Wilderspin, A. F., Trinnaman, B. J., & Green, N. M. (1982) *FEBS Lett. 146*, 87–92.

Post, R. L., & Sen, A. K. (1967) *Methods Enzymol. 10*, 773–776.

Scofano, H. M., Vieyra, A., & de Meis, L. (1979) *J. Biol. Chem. 254*, 10227–10231.

Seebregts, C. J., & McIntosh, D. B. (1989) *J. Biol. Chem. 264*, 2043–2052.

Suzuki, H., Obara, M., Kuwayama, H., & Kanazawa, T. (1987) *J. Biol. Chem. 262*, 15448–15456.

Takakuwa, Y., & Kanazawa, T. (1982) *J. Biol. Chem. 257*, 10770–10775.

Taylor, J. S., & Hattan, D. (1979) *J. Biol. Chem. 254*, 4402–4407.

Verjovski-Almeida, S., & Inesi, G. (1979) *J. Biol. Chem. 254*, 18–21.

Watanabe, T., & Inesi, G. (1982) *J. Biol. Chem. 257*, 11510–11516.

Yamamoto, T., & Tonomura, Y. (1967) *J. Biochem. (Tokyo) 62*, 558–575.